

\*\*Volume Title\*\*  
*ASP Conference Series, Vol. \*\*Volume Number\*\**  
 \*\*Author\*\*  
 © \*\*Copyright Year\*\* *Astronomical Society of the Pacific*

## Models of Stars, Brown Dwarfs and Exoplanets

Allard, F., Homeier, D., Freytag, B.

*CRAL, UMR 5574, CNRS, Université de Lyon, École Normale Supérieure de Lyon, 46 Allée d'Italie, F-69364 Lyon Cedex 07, France*

**Abstract.** Within the next few years, GAIA and several instruments aiming at imaging extrasolar planets will see first light. In parallel, low mass planets are being searched around red dwarfs which offer more favourable conditions, both for radial velocity detection and transit studies, than solar-type stars. Authors of the model atmosphere code which has allowed the detection of water vapour in the atmosphere of Hot Jupiters review recent advancement in modelling the stellar to substellar transition. The revised solar oxygen abundances and cloud model allow for the first time to reproduce the photometric and spectroscopic properties of this transition. Also presented are highlight results of a model atmosphere grid for stars, brown dwarfs and extrasolar planets.

### 1. Introduction

Since spectroscopic observations of very low mass stars (late 80s), brown dwarfs (mid 90s) and extrasolar planets (mid 2000s) are available, one of the most important challenges in modelling their atmospheres and spectroscopic properties lies in high temperature molecular opacities and cloud formation. K dwarfs show the onset of formation metal hydrides (starting around  $T_{\text{eff}} \sim 4500$  K), TiO and CO (below  $T_{\text{eff}} \sim 4000$  K), while water vapour forms in early M dwarfs ( $T_{\text{eff}} \sim 3900 - 2000$  K), and methane, ammonia and carbon dioxide are detected in late-type brown dwarfs ( $T_{\text{eff}} \sim 300 - 1600$  K) and in extrasolar giant planets. The latter are either observed by transit ( $T_{\text{eff}} \sim 1000 - 2000$  K depending on the spectral type of the central star and the distance to the star) or by imaging (young planets of  $T_{\text{eff}} \sim 300 - 2000$  K depending on their mass and age).

The modelling of the atmospheres of very low mass stars (hereafter VLMs) has evolved (as here illustrated with the development of the PHOENIX atmosphere code, which has allowed the detection of water vapour in extrasolar planets' atmospheres by Barman et al. 2007, 2008) with the extension of computing capacities from an analytical treatment of the transfer equation using moments of the radiation field (Allard 1990), to a line-by-line opacity sampling in spherical symmetry (Allard et al. 1997; Hauschildt et al. 1999a,b), and more recently to 3D radiation transfer (Seelmann et al. 2010). In parallel to detailed radiative transfer in an assumed static environment, hydrodynamical simulations have been developed to reach a realistic representation of the granulation and its induced line shifts for the sun and sun-like stars (see Freytag et al. 2011) by using a non-grey (multi-group binning of opacities) radiative transfer with a pure blackbody source function (scattering is neglected).

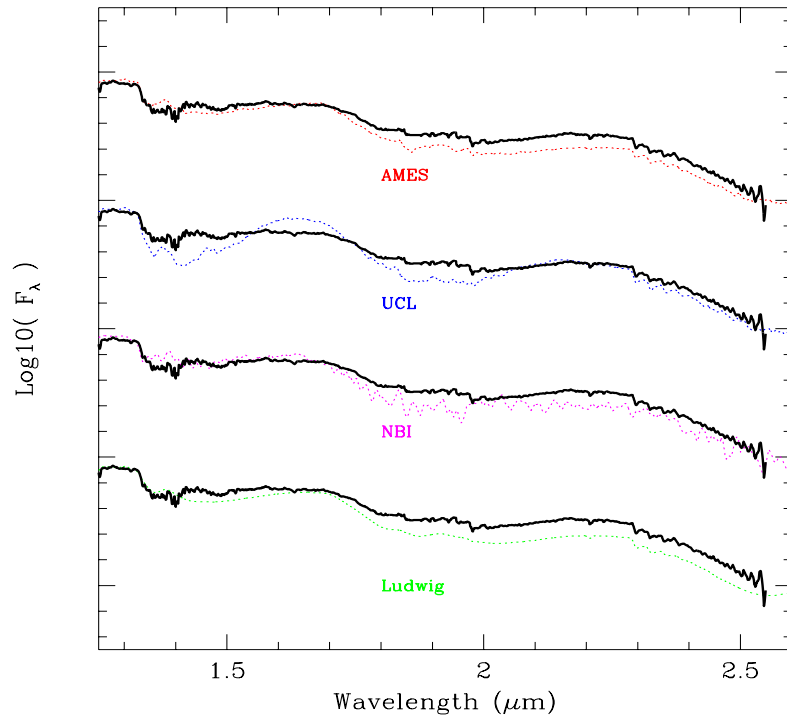


Figure 1. Synthetic spectra compared to the IR SED of VB10 using identical model parameters ( $T_{\text{eff}} = 2800\text{ K}$ ,  $\log g = 5.0$ ) and a resolution of  $50\text{ \AA}$  with different water vapour opacity sources: the Base grid by Allard & Hauschildt (1995) using Ludwig (1971); a test using the 1994 version of the Niels Bohr Institute (Jørgensen et al. 2001); the NextGen grid by Allard et al. (1994, 1997) and Hauschildt et al. (1999a,b) using the University College London database (Schryber et al. 1995); and the AMES-Cond/Dusty grid by Allard et al. (2000); Allard et al. (2001) using the NASA-Ames Center database (Partridge & Schwenke 1997). All models (except the NextGen/UCL case) underestimate the flux at  $K$  (ca.  $2.0 - 2.4\text{ }\mu\text{m}$ ) by 0.1 to 0.2 dex.

## 2. Molecular opacities

While earlier work has been developed for the study of red giant stars, the pioneering work on the modelling of VLM atmospheres has been provided by Mould (1975), Allard (1990) and Kui (1991) using a band model or Just Overlapping Line Approximation (JOLA) opacities developed by Kivel et al. (1952) and adapted for astrophysical use by Golden (1967). More realistic model atmospheres and synthetic spectra for VLMs, brown dwarfs and extrasolar planets have been made possible thanks to the development of accurate opacities calculated often ab initio for atmospheric layers where temperatures can reach 3000 K. The process of improvements was especially remarkable in the case of water vapour line lists. Indeed, water vapour has seen an important evolution through the years from band model approximations to straight means based on hot flames experiments, and then to ab initio computations. Nevertheless, the atmosphere models have failed to reproduce the strength of the water bands that shape the low resolution ( $R \leq 300$ ) infrared spectral energy distributions of M dwarfs. At the lower temperatures of brown dwarfs methane and ammonia rival the effect of water.

The discrepancies in the model synthetic spectra were therefore believed to be due to inaccurate or incomplete molecular opacities. In particular water vapour was suspected because the discrepancies were observed at infrared wavelengths in the relative brightnesses of the flux peaks between water vapour bands. As can be seen from Fig. 1 where the models are compared to the infrared spectrum of the M8e dwarf VB10, the water vapour opacity profile which shape this part of the spectrum has strongly changed over time with the improvement of computational capacities and a better knowledge of the interaction potential surface. And the most recent ab initio results confirm the earliest hot flames laboratory experiment results by Ludwig (1971). But in general, most opacity profiles produce an excess opacity (or lack of flux in the model) in the  $K$  bandpass. Only the UCL1994 line list (due to incompleteness, and with much of its deviations cancelling out over the bandpasses) could produce seemingly correct  $J - K_s$  colours.

### 3. The revised solar abundances

Model atmospheres for VLMs and in general for other stars assume scaled solar abundances for all heavy elements, with some enrichment of  $\alpha$ -process elements (the result of a "pollution" of the star-forming gas by the explosion of a supernova) when appropriate in the case of metal-depleted subdwarfs of the Galactic thick disk, halo and globular clusters. The revision of the solar abundances based on radiation hydrodynamical simulations of the solar atmosphere, on improvements in the quality of the spectroscopic observations of the Sun, and in its detailed line profile analysis by two separate groups using independent hydro codes and spectral synthesis codes (Asplund et al. 2009; Caffau et al. 2011) yield an oxygen reduction of 0.11–0.19 dex (up to 34%) compared to the previously used abundances of Grevesse et al. (1993). Since the overall SED of late K dwarfs, M dwarfs, brown dwarfs, and exoplanets is governed by oxygen compounds (TiO, VO in the optical and water vapour and CO in the infrared), the input elemental oxygen abundance used in the equation of state is of major importance. Fig. 2 shows an example of these effects for the optical and infrared SED of the M5.5 dwarf system Gl 866. However at other effective temperatures even stronger photometric effects can be seen, where the near-IR SED of different models diverges more (see Fig. 3). The comparison shows significant improvement compared to older models shown in Fig. 1, except for excess flux in the  $H$  bandpass near  $1.7 \mu\text{m}$  due to incomplete FeH opacity data for this region. The comparison has particularly improved in the Wing Ford band of FeH near  $0.99 \mu\text{m}$ , and in the VO bands thanks to line lists provided by B. Plez (GRAAL, Montpellier, France), although inaccurate or incomplete opacities are still affecting the models at optical wavelengths (e.g. the TiO line list by Langhoff 1997).

Fig. 3 compares the theoretical isochrones (assuming an age of 5 Gyrs) to the Casagrande et al. (2008)  $T_{\text{eff}}$  estimates and reveals that the NextGen models (Allard et al. 1997; Hauschildt et al. 1999a,b) systematically and increasingly overestimate  $T_{\text{eff}}$  through the lower main sequence, while the AMES-Cond/Dusty (Allard et al. 2001) models on the contrary underestimate  $T_{\text{eff}}$  as a function of  $J - K_s$  colour. This situation is relieved when using the current models (labeled BT-Settl in the figure) based on the revised solar abundances, and the models now agree fairly well with most of the empirical estimations of  $T_{\text{eff}}$ . The current model atmospheres have not yet been used as surface boundary condition to interior and evolution calculations, and simply provide the synthetic colour tables interpolated on the published theoretical isochrones (Baraffe et al.

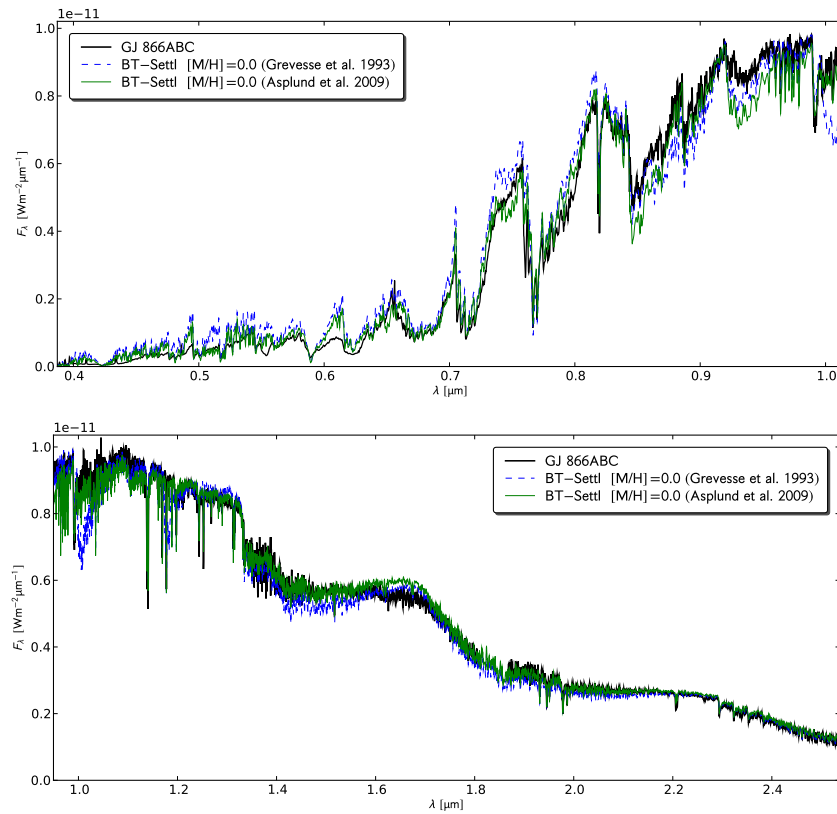


Figure 2. A BT-Settl synthetic spectrum with  $\log g=5.0$ , and solar metallicity by Asplund et al. (2009) is shown as light solid line, compared to the combined SED of the red dwarf triple system GJ 866 (Leinert et al. 1990; Delfosse et al. 1999). The observations were combined from a Mt. Stromlo optical spectrum (M. Bessell, priv. comm.) and SpeX infrared spectrum taken at the NASA IRTF (Rayner et al. 2009) (thick curve). For comparison a model using the same parameters and physical setup with the Grevesse et al. (1993) abundances is shown as a dashed line. The models have been scaled to the observed absolute flux assuming two equal  $T_{\text{eff}}=2920\text{ K}$  components of 0.157 solar radii and a third with  $T_{\text{eff}}=2700\text{ K}$  and  $0.126 R_{\odot}$ .

1998). Even if the atmospheres partly control the cooling and evolution of M dwarfs (Chabrier & Baraffe 1997), differences introduced in the surface boundary conditions by changes in the model atmosphere composition have negligible effect.

#### 4. Cloud formation

One of the most important challenges in modelling these atmospheres (below 2600K) is the formation of clouds. Tsuji et al. (1996) had identified dust formation by recognising the condensation temperatures of hot dust grains (enstatite, forsterite, corundum:  $\text{MgSiO}_3$ ,  $\text{Mg}_2\text{SiO}_4$ , and  $\text{Al}_2\text{O}_3$  crystals) to occur in the line-forming layers ( $\tau \approx 10^{-4} - 10^{-2}$ ) of their atmospheres. The cloud composition, according to equilibrium chemistry, is going from zirconium oxide ( $\text{ZrO}_2$ ), to refractory ceramics (per-

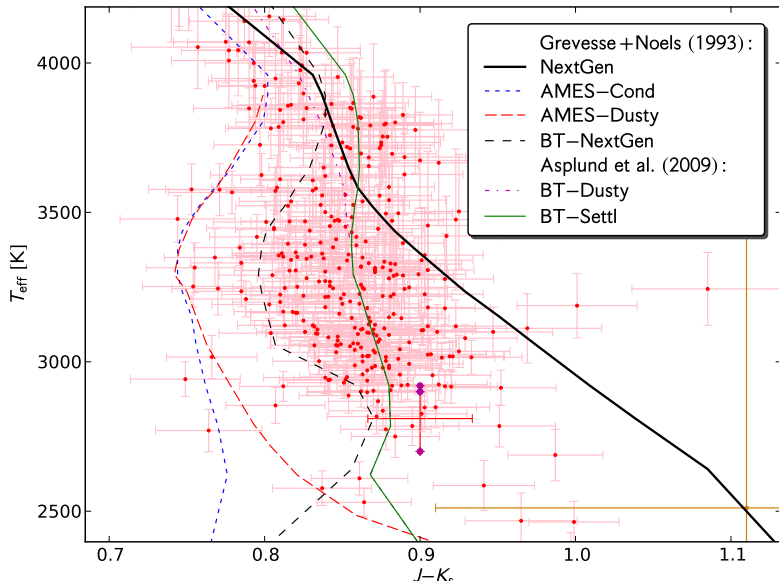


Figure 3. Estimated  $T_{\text{eff}}$  for M dwarfs by Casagrande et al. (2008) and brown dwarfs by Golimowski et al. (2004); Vrba et al. (2004) are compared to the NextGen isochrones for 5 Gyrs (Baraffe et al. 1997, 1998) using various generations of model atmospheres: NextGen (thick line), the limiting case AMES-Cond/Dusty cases by Allard et al. (2001) (dotted and dashed lines), the current BT-Settl models using the Asplund et al. (2009) solar abundances (full line). The Gl 866 system fitted in Fig. 2 is highlighted by darker colours and shown with its relatively large photometric error bars at  $J - K_s = 0.9$ .

ovskite and corundum;  $\text{CaTiO}_3$ ,  $\text{Al}_2\text{O}_3$ ), to silicates (e.g. forsterite;  $\text{Mg}_2\text{SiO}_4$ ), to salts (CsCl, RbCl, NaCl), and finally to ices ( $\text{H}_2\text{O}$ ,  $\text{NH}_3$ ,  $\text{NH}_4\text{SH}$ ) as brown dwarfs cool down over time from M through L, T, and Y spectral types (Allard et al. 2001; Lodders & Fegley 2006). This assumed (by Allard et al. 2001) sub-micron-sized crystal formation causes the weakening and vanishing of TiO and VO molecular bands (via  $\text{CaTiO}_3$ ,  $\text{TiO}_2$ , and  $\text{VO}_2$  grains) from the optical spectra of late M and L dwarfs, revealing CrH and FeH bands otherwise hidden by the molecular pseudo-continuum, and the resonance doublets of alkali transitions which are only condensing onto salts in late-T dwarfs. The scattering effects of this fine dust is Rayleigh scattering which provides veiling to the optical SED of late-M and L dwarfs, while the greenhouse effect due to the dust cloud causes their infrared colours to become extremely red compared to those of hotter low mass stars. The upper atmosphere, above the cloud layers, is depleted from condensable material and significantly cooled down by the reduced or missing pseudo-continuum opacities.

One common approach has been to explore the limiting properties of cloud formation. One limit is the case where sedimentation or gravitational settling is assumed to be fully efficient such as the case B of Tsuji (2002), the AMES-Cond or condensed phase models of Allard et al. (2001), the clear case of Ackerman & Marley (2001) and the cloud-free case of Burrows et al. (2006). The other limit is the case where gravitational settling is assumed inefficient and dust, often only forsterite, forms in equilibrium with the gas phase such as the case A of Tsuji (2002), the AMES-Dusty or dusty models of Allard et al. (2001), the cloudy case of Ackerman & Marley (2001), or the case B of

Burrows et al. (2006). These limiting cases of maximum dust content agree in describing the evolution of brown dwarfs from a molecular opacity governed SED towards a blackbody SED below 1500K. This description was suitable, at least in the case of the AMES-Dusty models, in reproducing the infrared colours of L dwarfs. The cloud-free limiting case on the other hand allowed to reproduce to some degree the colours of T dwarfs. Fig. 4 shows this situation for the AMES-Cond/Dusty limiting case models of Allard et al. (2001) compared with the effective temperatures estimates obtained by integration of the observed SED (Golimowski et al. 2004; Vrba et al. 2004).

The purpose of a cloud model is therefore to go beyond these limiting cases and define the number density and size distribution of condensates as a function of depth in the atmosphere. The discovery of dust clouds in M dwarfs and brown dwarfs has therefore triggered the development of cloud models building up on pioneering work in the context of planetary atmospheres developed by Lewis (1969), Rossow (1978), and Lunine et al. (1989). The Lewis model is an updraft model (considering that condensation occurs in a gas bubble that is advected from deeper layers). By lack of knowledge of the velocity field and diffusion coefficient of condensates in the atmospheres of the planets of the solar system, Lewis simply assumed that the advection velocity is equal to the sedimentation velocity, thereby preserving condensable material in the condensation layers. This cloud model did not account for grain sizes. Rossow on the other hand developed characteristic timescales as a function of particle size for the main microphysical processes involved (condensation, coagulation, coalescence, and sedimentation). The intersections of these characteristic timescales gives an estimate of the condensate number densities and mean grain sizes. However, this model made several explicit assumptions concerning the efficiency of supersaturation, the coagulation, etc.

Helling et al. (2008a) have compared different cloud models and their impact on model atmospheres. Most cloud models define the cloud base as the evaporation layer provided by the equilibrium chemistry. In the unified cloud models of Tsuji (2002); Tsuji et al. (2004) a parametrization of the radial location of the cloud top by way of an adjustable parameter  $T_{\text{crit}}$  was used. This choice permits to determine the cloud extension effects on the spectra of these objects but does not allow to reproduce the stellar-substellar transition with a unique value of  $T_{\text{crit}}$  since the cloud extension depends on the atmospheric parameters.

Allard et al. (2003) using PHOENIX and the index of refraction of up to 40 condensable species, have applied the Rossow cloud model, ignoring coalescence and coagulation, and comparing the timescales of condensation, sedimentation and mixing (extrapolated from the convective velocities into the convectively stable layers), and assuming efficient nucleation (monomers equilibrium densities). The cloud model was then solved layer by layer inside out to account for the sequence of grain species formation as a function of cooling of the gas. But this version of the BT-Settl (with gravitational settling) models did not allow for the formation of enough dust in brown dwarf atmospheres due to a too conservative prescribed supersaturation value.

Ackerman & Marley (2001) have solved the particle diffusion problem of condensates assuming a parametrized sedimentation efficiency  $f_{\text{sed}}$  (constant through the atmosphere) and a mixing assumed constant and fixed to its maximum value (maximum of the inner convection zone). Saumon & Marley (2008) found that their models could not produce the color change with a single value of  $f_{\text{sed}}$ .

Helling et al. (2008b) use the PHOENIX code to compute the Drift-Phoenix models. The cloud model used, in the contrary to all other cases mentioned, studies the

nucleation and growth of grains as they sediment down into the atmosphere. This cloud model determines the number density and size distribution of grains by 1D nucleation simulations, and the resulting distribution is read in by PHOENIX which computes the resulting opacities and radiative transfer. These models solve the nucleation problem but only for the assumed monomer types and have been successfully applied to fit the dusty atmospheres of L dwarfs, but the reversal in IR colours observed for the L/T transition could not be explained (Witte et al. 2011).

None of these models however treated the mixing properties of the atmosphere and the resulting diffusion mechanism realistically enough to reproduce the brown dwarf spectral transition without changing cloud parameters. Freytag et al. (2010) have therefore addressed the complementary though important issue of mixing and diffusion in these atmospheres by 2D radiation hydrodynamic (hereafter RHD) simulations, using the PHOENIX gas opacities in a multi-group opacity scheme, and forsterite with geometric cross-sections. These simulations assume efficient nucleation, using monomer densities estimated from the total available density of silicon (least abundant element in the solar composition involved in forsterite). They found that gravity waves play a decisive role in clouds formation, while around  $T_{\text{eff}} \leq 2200$  K the cloud layers become optically thick enough to initiate cloud convection, which participate in the mixing. Overshoot can also be important in the deepest layers.

These RHD simulations allow an estimation of the diffusion processes bringing fresh condensable material from the hotter lower layers to the cloud forming layers. We have therefore updated our cloud model (BT-Settl models) to account for the mixing prescribed by the RHD simulations. Another important improvement concerns the supersaturation which as been computed rather than using the fixed conservative value recommended by Rossow. One can see from Fig. 4 that the late-type M and early-type L dwarfs behave as if dust is formed nearly in equilibrium with the gas phase with extremely red colours in some agreement with the BT-Dusty models. The BT-Settl models reproduce the main sequence down to the L-type brown dwarf regime, subjected in the  $K$  bandpass to the greenhouse effect of dust clouds, before turning to the blue in the late-L and T dwarf regime as a result of methane formation in the  $K$  bandpass. This constitutes a major improvement over previous models, and is promising that we can reach in the near future a full explanation of the stellar substellar transition.

Diffusion has also been held responsible for deviations in ultracool atmospheres from gas phase chemical equilibrium (CE), as noted in early observations of T dwarfs showing an excess of carbon monoxide absorption (Noll et al. 1997; Griffith & Yelle 1999). More recently, carbon dioxide (Tsuiji et al. 2011), which was not expected at such low temperatures, has been detected. Similarly, ammonia has been shown to be underabundant (Saumon et al. 2006). This is understood as the result of slowing down of crucial chemical reaction steps, so that some important molecules ( $\text{CH}_4$ ,  $\text{NH}_3$ ) would not have the time to form in equilibrium while undergoing mixing, whereas others ( $\text{CO}$ ,  $\text{CO}_2$ ,  $\text{N}_2$ ) remain at enhanced abundances. The RHD simulations of Freytag et al. (2010) have allowed to understand the underlying mixing processes, obviating the need to describe them with an additional free parameter.

## 5. Applications to Exoplanet Science

Several infrared integral field spectrographs combined with coronograph and adaptive optic instruments being developed are coming online before 2013 (SPHERE at the VLT,

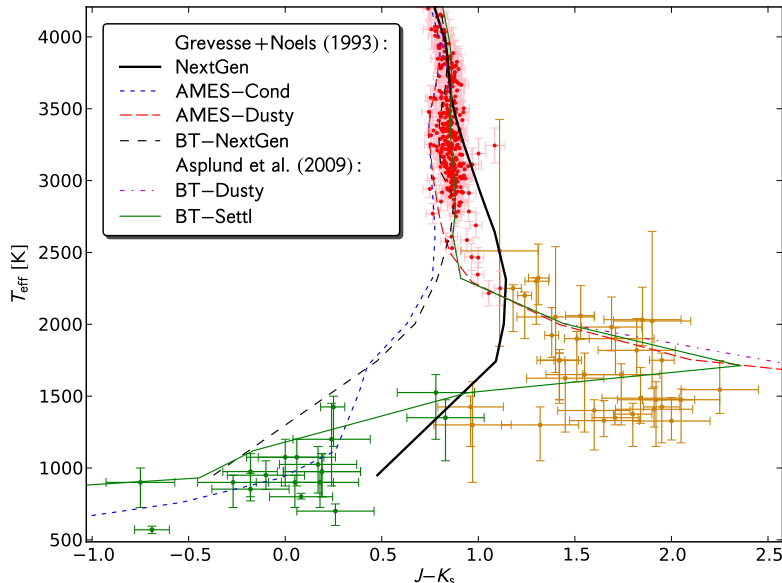


Figure 4. Same plot as Fig. 3 but zooming out and extending into the brown dwarf region of the diagram. This region below 2500K is dominated by dust formation (essentially forsterite and other silicates). The limiting cases AMES-Cond/Dusty model atmospheres provide a description of the span in colours of the brown dwarfs in this diagram for a given age (here 5 Gyrs). The BT-Settl models succeed in explaining even the most extreme colours of brown dwarfs.

the Gemini Planet Imager at Gemini south, Project 1640 at Mount Palomar, etc.). The E-ELT 41m telescope in Spain due around 2020 will also be very ideally suited for planet imaging. The models developed for VLMs and brown dwarfs are a unique opportunity, if they can explain the stellar-substellar transition, to provide a great support for the characterisation of imaged exoplanets. We have therefore developed the BT-Settl model atmosphere grid to encompass the parameter regime of these objects (surface gravity around  $\log g=4.0$ ,  $T_{\text{eff}}$  below 2000K).

These planets are typically found at several dozens of AU from the star, and since the observations are done in the infrared the non-irradiated models can even be used directly. Indeed, Barman et al. (2001) have shown that the effects of impinging radiation from a star on the planetary atmosphere are Rayleigh scattering of the stellar light by  $\text{H}_2$  molecules (or clouds if present) at optical wavelengths (below 1  $\mu\text{m}$  for solar type stars), while the impact on the interior and evolution properties becomes negligible for orbital distances exceeding 0.1 AU. Nevertheless, we are developing for 2012 irradiated models and the capacity to compute them via the PHOENIX simulator (see below).

## 6. Summary and Future Prospects

We report progress of the development of a new model atmosphere grid for stars, brown dwarfs and young planets, named BT-Settl. It has been computed using the PHOENIX code updated for: i) the Barber et al. (2006) BT2 water, the Homeier et al. (2003) STDS methane, the Sharp & Burrows (2007) ammonia and the Tashkun et al. (2004) CDSD-1000  $\text{CO}_2$  opacity line lists, ii) the solar abundances revised by Asplund et al. (2009),

and iii) a cloud model accounting for more detailed supersaturation and RHD mixing. The grid is covering the whole range of stars to young planets  $400 \text{ K} < T_{\text{eff}} < 70,000 \text{ K}$ ;  $-0.5 < \log g < 5.5$ ; and  $-4.0 < [\text{M}/\text{H}] < +0.5$ , including values of the  $\alpha$ -element enhancement (supernovae enrichment of the star forming material) between  $+0.0$  and  $+0.6$ . Models are available at the PHOENIX simulator website <http://phoenix.ens-lyon.fr/simulator/> and are in preparation for publication to serve among others the GAIA, MUSE and SPHERE/GPI/P1640 instruments to come online in the near future. Corresponding evolution models are expected for 2012.

We found the previously used NextGen models to systematically overestimate  $T_{\text{eff}}$  below 3500 K by as much as 500 K. The water vapour opacity profile has converged with the most recent line lists reproducing laboratory results, but could not explain this discrepancy. The solution came instead from the revision of the solar abundances which changes the strength of the water vapour absorption bands, and therefore allows the reproduction of the spectroscopic and photometric properties of M dwarfs as late as M6. Later-type M dwarfs are affected by dust formation and cloud modelling is important to understand their properties. We find that the Rossow cloud model allows, with revisions to the supersaturation and mixing, the reproduction of the stellar-substellar transition. A small offset persists however in the M-L transition. It is possible that all the current cloud models are not efficient enough in producing dust at the onset of cloud formation regime. Detailed nucleation studies could allow in the future to resolve this issue. Other uncertainties affect the current cloud modelling such as the assumption of spherical non-porous grains while grains form as fractals in the laboratory. Constraining the models remains therefore very important.

Beyond cloud modelling and molecular opacities, model atmospheres for these objects require reaction rates for the most abundant molecules and/or most important absorbers. Furthermore, these atmospheres are composed of molecular hydrogen which constitute the main source of collisions. Also needed are therefore collision rates (by  $\text{H}_2$ ) and corresponding damping constants for the broadening molecular lines.

In order to say something about the spectral variability of VLMs, brown dwarfs and planets, 3D global or "star in a box" RHD simulations with rotation will be required. This is our current project supported by the French "Agence Nationale de la Recherche" for the period 2010-2015.

**Acknowledgments.** We thank the French "Agence Nationale de la Recherche" (ANR), and the "Programme National de Physique Stellaire" (PNPS) of CNRS (INSU) for their financial support. The computations of dusty M dwarf and brown dwarf models were performed at the *Pôle Scientifique de Modélisation Numérique* (PSMN) at the *École Normale Supérieure* (ENS) in Lyon and at the *Gesellschaft für Wissenschaftliche Datenverarbeitung Göttingen* in collaboration with the Institut für Astrophysik Göttingen.

## References

Ackerman, A. S., & Marley, M. S. 2001, ApJ, 556, 872  
 Allard, F. 1990, Ph.D. thesis, Ruprecht Karls Univ. Heidelberg  
 Allard, F. et al. 2001, ApJ, 556, 357  
 — 2003, in Brown Dwarfs, edited by E. Martín, vol. 211 of IAU Symposium, 325  
 Allard, F., & Hauschildt, P. H. 1995, ApJ, 445, 433  
 Allard, F., Hauschildt, P. H., Alexander, D. R., & Starrfield, S. 1997, ARA&A, 35, 137  
 Allard, F., Hauschildt, P. H., Miller, S., & Tennyson, J. 1994, ApJ, 426, L39  
 Allard, F., Hauschildt, P. H., & Schwenke, D. 2000, ApJ, 540, 1005  
 Asplund, M., Grevesse, N., Sauval, A. J., & Scott, P. 2009, ARA&A, 47, 481

Baraffe, I., Chabrier, G., Allard, F., & Hauschildt, P. H. 1997, *A&A*, 327, 1054  
 — 1998, *A&A*, 337, 403

Barber, R. J., Tennyson, J., Harris, G. J., & Tolchenov, R. N. 2006, *MNRAS*, 368, 1087

Barman, T. 2007, *ApJ*, 661, L191

Barman, T. S. 2008, *ApJ*, 676, L61

Barman, T. S., Hauschildt, P. H., & Allard, F. 2001, *ApJ*, 556, 885

Burrows, A., Sudarsky, D., & Hubeny, I. 2006, *ApJ*, 640, 1063

Caffau, E., Ludwig, H.-G., Steffen, M., Freytag, B., & Bonifacio, P. 2011, *Solar Phys.*, 268, 255

Casagrande, L., Flynn, C., & Bessell, M. 2008, *MNRAS*, 389, 585

Chabrier, G., & Baraffe, I. 1997, *A&A*, 327, 1039

Delfosse, X., Forveille, T., Udry, S., Beuzit, J.-L., Mayor, M., & Perrier, C. 1999, *A&A*, 350, L39

Freytag, B., Allard, F., Ludwig, H., Homeier, D., & Steffen, M. 2010, *A&A*, 513, A19+

Freytag, B., Steffen, M., Ludwig, H.-G., Wedemeyer-Böhm, S., Schaffenberger, W., & Steiner, O. 2011, *J. Comp. Phys.*, 10.1016/j.jcp.2011.09.026

Golden, S. A. 1967, *J. Quant. Spec. Radiat. Transf.*, 7, 225

Golimowski, D. A. et al. 2004, *AJ*, 127, 3516

Grevesse, N., Noels, A., & Sauval, A. J. 1993, *A&A*, 271, 587

Griffith, C. A., & Yelle, R. V. 1999, *ApJ*, 519, L85

Hauschildt, P. H., Allard, F., & Baron, E. 1999a, *ApJ*, 512, 377

Hauschildt, P. H., Allard, F., Ferguson, J., Baron, E., & Alexander, D. R. 1999b, *ApJ*, 525, 871

Helling, C., Ackerman, A., Allard, F., Dehn, M., Hauschildt, P., Homeier, D., Lodders, K., Marley, M., Rietmeijer, F., Tsuji, T., & Woitke, P. 2008a, *MNRAS*, 391, 1854

Helling, C., Dehn, M., Woitke, P., & Hauschildt, P. H. 2008b, *ApJ*, 675, L105

Homeier, D., Hauschildt, P. H., & Allard, F. 2003, in *Stellar Atmosphere Modeling*, edited by I. Hubeny, D. Mihalas, & K. Werner, vol. 288 of *ASP Conference Series*, 357

Jørgensen, U. G., Jensen, P., Sørensen, G. O., & Aringer, B. 2001, *A&A*, 372, 249

Kivel, B., Mayer, H., & Bethe, H. 1952, *Ann. Phys.*, 2, 57

Kui, R. 1991, Ph.D. thesis, National University Australia

Langhoff, S. R. 1997, *ApJ*, 481, 1007

Leinert, C., Haas, M., Allard, F., Wehrse, R., McCarthy, D. W., Jahreiss, H., & Perrier, C. 1990, *A&A*, 236, 399

Lewis, J. S. 1969, *Icarus*, 10, 365

Lodders, K., & Fegley, B., Jr. 2006, *Chemistry of Low Mass Substellar Objects* (Springer Verlag), 1

Ludwig, C. B. 1971, *Appl. Optics*, 10, 1057

Lunine, J. I., Hubbard, W. B., Burrows, A., Wang, Y.-P., & Garlow, K. 1989, *ApJ*, 338, 314

Mould, J. R. 1975, *A&A*, 38, 283

Noll, K. S., Geballe, T. R., & Marley, M. S. 1997, *ApJ*, 489, L87+

Partridge, H., & Schwenke, D. W. 1997, *J. Comp. Phys.*, 106, 4618

Rayner, J. T., Cushing, M. C., & Vacca, W. D. 2009, *ApJS*, 185, 289

Rossow, W. B. 1978, *ICARUS*, 36, 1

Saumon, D., & Marley, M. S. 2008, *ApJ*, 689, 1327

Saumon, D., Marley, M. S., Cushing, M. C., Leggett, S. K., Roellig, T. L., Lodders, K., & Freedman, R. S. 2006, *ApJ*, 647, 552

Schryber, J. H., Miller, S., & Tennyson, J. 1995, *JQSRT*, 53, 373

Seelmann, A. M., Hauschildt, P. H., & Baron, E. 2010, *A&A*, 522, A102+

Sharp, C. M., & Burrows, A. 2007, *ApJS*, 168, 140

Tashkun, S. A., Perevalov, V. I., Teffo, J.-L., Bykov, A. D., Lavrentieva, N. N., & Babikov, Y. L. 2004, vol. 5311 of *SPIE Conference Series*, 102

Tsuji, T. 2002, *ApJ*, 575, 264

Tsuji, T., Nakajima, T., & Yanagisawa, K. 2004, *ApJ*, 607, 511

Tsuji, T., Ohnaka, K., & Aoki, W. 1996, *A&A*, 305, L1

Tsuji, T., Yamamura, I., & Sorahana, S. 2011, *ApJ*, 734, 73

Vrba, F. J. et al. 2004, *AJ*, 127, 2948

Witte, S., Helling, C., Barman, T., Heidrich, N., & Hauschildt, P. H. 2011, A&A, 529, A44